17th World Conference on Earthquake Engineering, 17WCEE
Sendai, Japan - September 13th to 18th 2020

PERFORMANCE OF ORTHOGONAL DIRECTION ON CONTINUOUS BEAM TYPE CFST BEAM-TO-COLUMN CONNECTION

T. Fujinaga[(1)], C. G. Clifton[(2)]

[(1)] *Associate Professor, Kobe University, ftaka@kobe-u.ac.jp*
[(2)] *Associate Professor, University of Auckland, c.clifton@auckland.ac.nz*

Abstract

In order to simplify the fabrication requirements and costs of Concrete-filled steel tubular (CFST) beam-to-column connections, a continuous beam type connection through the column is proposed for I-beam to CFST column connections. These use I-section beams that pass through the CFST columns and are fixed in place with a fillet weld all round between the I-section beam and the outer faces of the column. Previous researchers have investigated the one-way action of continuous beam type CFST beam-to-column connection. This type of connection can readily develop the full plastic moment capacity of the beam. However, in a two-way configuration, the behaviour of the beam to column connection in the orthogonal direction to the continuous beam may not behave so well.

The authors have proposed a new beam-to-column connection detail for the orthogonal direction to the continuous beam (see Fig.1). Two specimens of 1) Continuous beam only and 2) Beam in orthogonal direction to the continuous beam have been planned.

In this paper, the experimental testing results of the two types of CFST beam-to-column connection specimens are presented and the connection performance and load transfer mechanisms are examined. The continuous beam type specimen demonstrated good seismic performance, exhibiting stable hysteretic behaviour with high energy absorption. The maximum experimental strength exceeded the calculated value. The orthogonal direction to continuous beam specimen showed slightly pinched hysteresis until R=0.01rad. However, it showed stable hysteretic behaviour thereafter, with an increased strength under high rotation. The increase of strength might be caused by the inserted beam web contacting the continuous beam flange, enabling a greater lever action to develop bending moment. The pinching effect could be reduced by reducing the clearance between the top and bottom of the coped web and the adjacent contact surface of the continuous beam flange.

Keywords: Concrete-filled steel tube; Plasma cutting; Fillet welding; Orthogonal direction; Local buckling

1. Introduction

Concrete-filled steel tubular (CFST) columns are used widely as building structure components because of their good structural performance under earthquake, fire and gravity loading and their ease of construction. Nevertheless, connecting beams into CFST columns can be especially complex when rigid beam-to-column connections are required. CFST beam-to-column connections are generally designed as thorough-diaphragm type, outer-diaphragm type, and inner-diaphragm type. Design formulas for these three types of beam-to-column connection are given in AIJ CFT Recommendations [1] and in similar recommendations for New Zealand.

In order to simplify the fabrication requirements and costs of these connections, a continuous beam type connection has been proposed for CFST beam-to-column connections that uses I-section beams passing through CFST columns [2]. This continuous beam type connection can easily develop the full plastic moment capacity of the steel beam and considerably simplify the design of the CFST beam-to-column connection. This type of connection can be built only using fillet welding, rather than requiring the complete penetration butt welding required in a conventional beam to diaphragm plate connection, which is critically dependent on the skill of the welder. For circular CFST columns, load transfer mechanism and design formulas are discussed, but few examples exist for square columns for CFST beam-to-column connections [3, 4]. The authors have conducted an experiment of continuous beam type square CFST beam-to-column connection, and indicated that filled concrete contributes to the transmission of the compressive load at the connection panel [5]. However, in the case of an orthogonal direction to the continuous beam, the orthogonal beam cannot pass through the column because the continuous beam exists. How to fix the orthogonal beam into the continuous beam/column connection is an issue as there is no research that examined the connection performance of an orthogonal direction to the continuous beam.

In this paper, a new beam-to-column connection detail for the orthogonal direction to the continuous beam was proposed. Following the previous paper [5], the experiment of two types of T-shaped CFST beam-to-column connection specimen was conducted. Two specimens of 1) Continuous beam type specimen and 2) Specimen of orthogonal direction to continuous beam have been planned. As described herein, the experiment testing results of two types of square CFST beam-to-column connection specimens are presented and the connection performance and load transfer mechanisms are examined.

2. Methodology

2.1 Specimens

The dimensions of the specimens are presented in Figure 1. Specimens are T-shaped and simulating the square CFST beam-to-column connection. Two specimens of 1) Continuous beam type specimen and 2) Orthogonal direction to continuous beam specimen have been planned and designed so that beam yields prior to other parts (See Table.1). Continuous beam type specimen required an I-section beam slot to be cut in column steel tube by plasma within 1mm tolerance. After putting the I-section beam through the slot, the I-section beam and outer faces of the column were fillet-welded all round. The details of orthogonal direction to continuous beam specimen is shown in Figure 2. For orthogonal direction to continuous beam specimen, a short beam which simulates continuous beam were arranged as a transverse beam. Inserted beam web was metal-touched to transverse continuous beam web, and clearance between the flange of transverse continuous beam and web of the inserted beam was about 1-2 mm.

The standard tensile and compressive tests were conducted for steel and concrete to ascertain the mechanical properties of the materials used. The measured results are presented in Tables 2. The relationship between the concrete material age and strength is portrayed in Figure 3.

Table 1 – Dimension of specimens

Specimen	Columns	Beam	Strength of concrete (MPa)
Continuous Beam Type	250x250x9 (BCR295)	H-300x150x6.5x9 (SN400B)	80.5
Orthogonal Direction to Continuous Beam			80.7

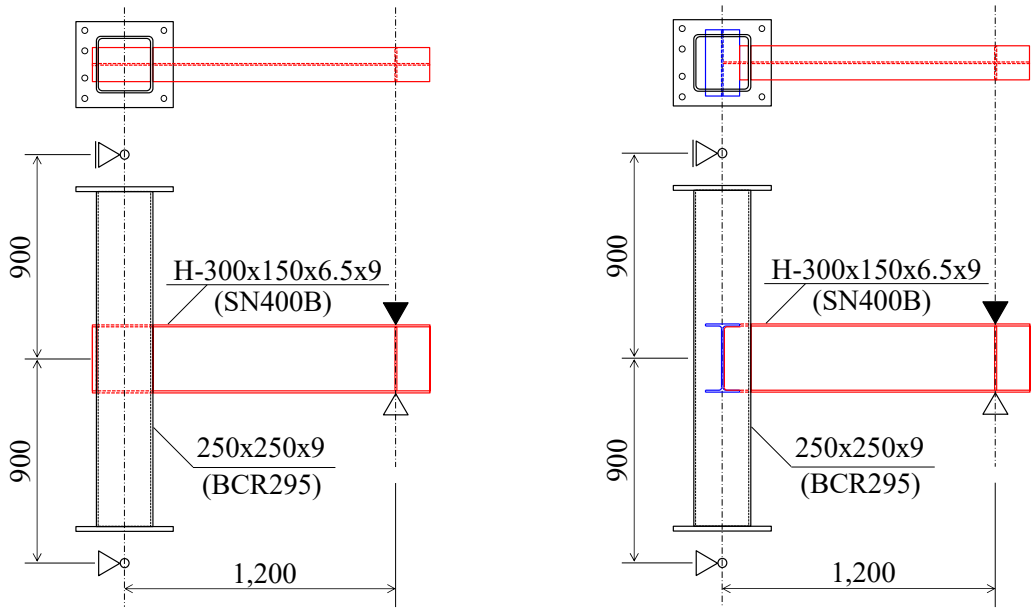

(a) Continuous beam type (b) Orthogonal direction to continuous beam

Fig. 1 – Dimensions of specimen

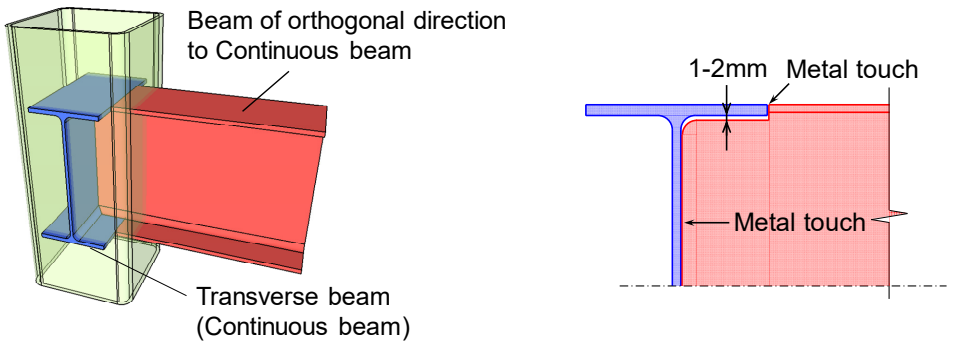

Fig. 2 – Detail of joint

Table 2 – Mechanical properties of steel

		$_sE$ (GPa)	f_y (MPa)	f_u (MPa)	Elongation (%)
Beam	I-section flange	178	322	482	40.4
	I-section web	190	362	486	24.8
Column	Steel Pipe	182	349	423	26.5

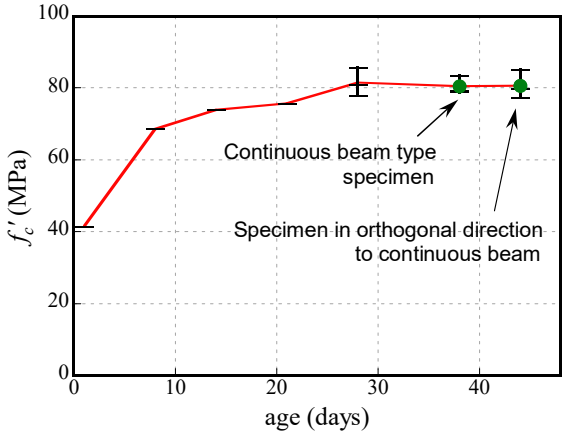

Fig. 3 – Change of concrete strength

2.2 Loading method

The top end of the specimens was supported by hinge and roller; the bottom end was supported by a hinge. Shear force was added by hydraulic jack set at beam end (See Figure 4). Stiffening devices for the displacement to the out-of-plane direction were set at top of the column and beam end. Loading was controlled by rotational angle and the targeted rotation angles were 0.005rad, 0.01rad, 0.02rad and 0.03rad. The rotation angle R was calculated using vertical displacement of beam end and the distance between loading point and column centre (1200 mm).

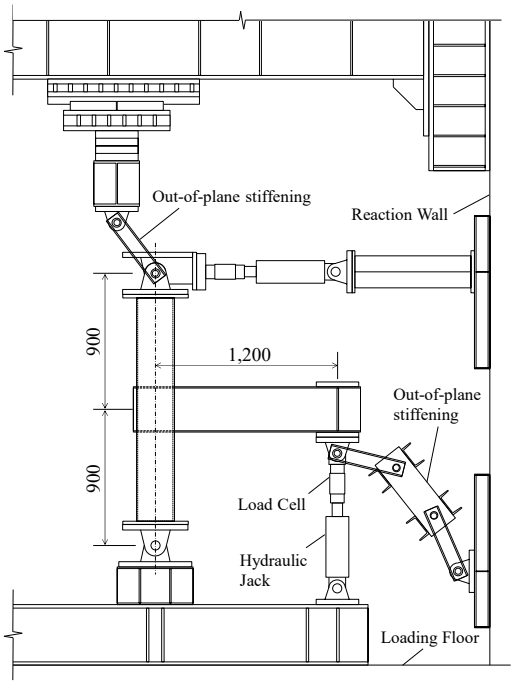

Fig. 4 – Loading apparatus

3. Experimental results

3.1 Shear force and rotation angle relation

Figure 5 presents the measured shear force – rotation angle relationships. The measured behaviour is shown as red solid lines. Black circles show the point at which beam flange began yielding. Arrows indicate points at which local buckling was observed at the I-section beam flange. Green and blue lines show shear forces calculated using yield flexural strength and ultimate flexural strength.

The continuous beam type specimen demonstrated good seismic performance exhibiting stable hysteretic behaviour with high energy absorption. Yielding of the beam flange was observed at R=0.01rad. Local buckling of upper and bottom beam flange was observed at R=0.02rad. The maximum experimental strength was observed at R=0.03rad. Photo 1(a) is portrayed the local buckling at steel beam-end after the loading test. Local buckling was not observed at the column flange until the end of loading, and there was no failure at fillet weld part.

The orthogonal direction to continuous beam specimen showed slightly pinched hysteresis until R=0.01rad and more gradual buildup of strength. However, it showed stable hysteretic behaviour thereafter, with an increased strength under high rotation. The increase of strength is expected to be caused by the inserted beam web contacting the continuous beam flange, enabling greater lever action to develop the bending moment. A crack was observed in the steel beam-end bottom weld at R=0.01rad. With the growth of crack, column flange was pulled by I-section beam flange with appreciable local deformation (see Photo 1(b)).

Table 3 presents the comparison between experimental data and calculated data. Calculated values of yield strength and maximum strength are derived using the flexural yield moment $\underline{M_y}$ and full plastic moment M_p. Regarding the continuous beam type specimen, the yield experimental value exceeded a calculated value by 10%, the maximum experimental value exceeded a calculated value by 35%. In the case of an orthogonal direction to continuous beam specimen, the failure mechanism was pulling off of the steel beam. So, it doesn't make much sense in the comparison between the experimental data and the calculated data, but the maximum experimental strength is almost the same as the calculated yield strength.

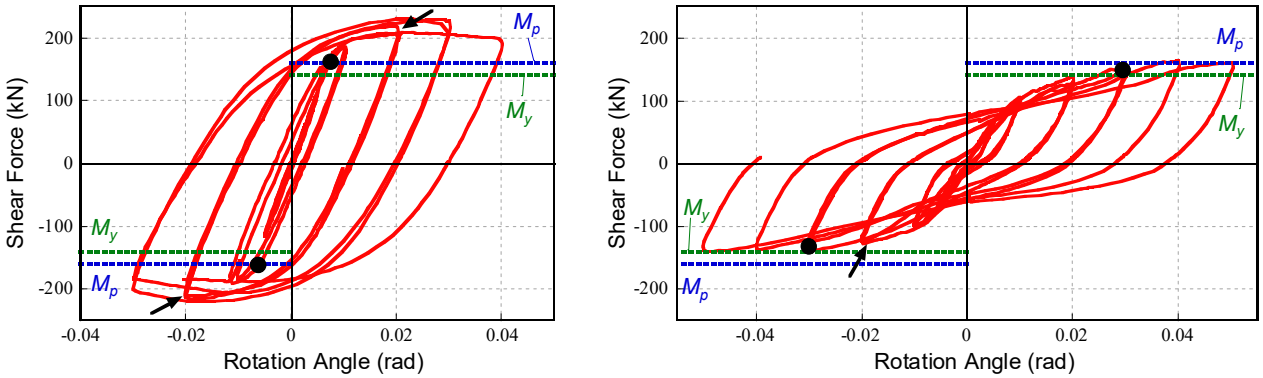

(a) Continuous Beam Type (b) Orthogonal Direction to Continuous Beam

Fig. 5 – Shear Force – Rotation Angle Relationship

Table 3 – Comparison between Test Results and Calculated Value

Specimen		Yield Strength (kN)			Ultimate Strength (kN)			Initial Stiffness (kN/rad)		
		Cal	Exp	Exp/Cal	Cal	Exp	Exp/Cal	Cal	Exp	Exp/Cal
Continuous Beam Type	+	144	162	1.13	162	231	1.42	19.2	22.1	1.15
	-		-161	-1.12		-219	-1.35			
Orthogonal Direction to Continuous Beam	+		150	1.04		164	1.01		15.0	0.78
	-		-137	-0.95		-139	-0.86			

(a) (b)

Photo 1 –Failure Mode of Specimens; (a) Local Buckling at Beam Flange (Continuous Beam Type Specimen), (b) Crack in Fillet Welding Part (Orthogonal Direction to Continuous Beam Specimen)

3.2 Deformation of I-section beam

Figure 6 shows the curvature distributions of I-section steel beam. The curvature was calculated using measured value of strain gauges put at top and bottom centre of I-section beam flange, and normalized by depth of I-section beam. The abscissa of the graph is the distance from surface of the column tube. Figure 7 presents the rotation angle at beam-end – rotation angle relationships. The rotation angle at the beam-end was measured using the displacement transducer set above and below the steel beam at150mm from the surface of the column flange.

In case of the continuous beam type specimen, curvature close to the column tube was increased with increase of rotation angle after R=0.01rad. The largest contribution to the rotation angle depends on the rotation of the beam end, and that indicates the beam collapse mechanism.

In case of the orthogonal direction beam to the continuous beam, the curvature of the I-section steel beam remained very small, as the overall rotation angle increased. It is clear however, stress was difficult to be transmitted to beam flange, because of the occurrence of crack in beam-end fillet welding part at R=0.01rad. The local buckling observed in the orthogonal steel beam was much smaller than that along the continuous beam type specimen.

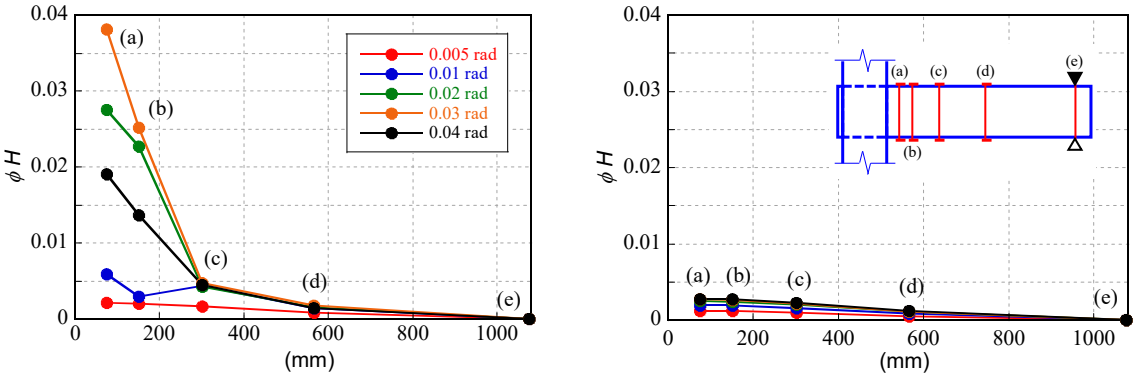

(a) Continuous Beam Type (b) Orthogonal Direction to Continuous Beam

Fig. 6 – Curvature Distributions of I-section Steel Beam

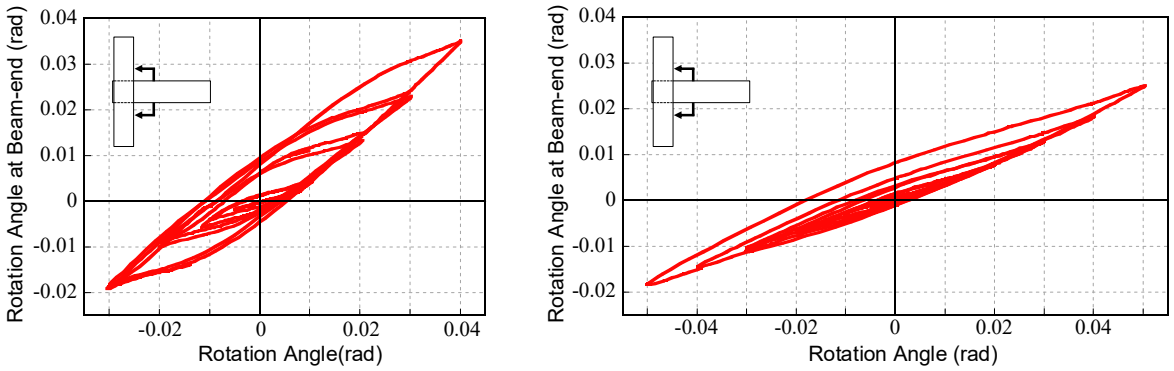

(a) Continuous Beam Type (b) Orthogonal Direction to Continuous Beam

Fig. 7 – Rotation Angle at Beam-end – Rotation Angle Relationship

3.3 Strain hysteresis

Figure 8 presents the strain distributions at the column flange above and below the steel beam. These strain gauges were located 25mm clear distance above the top of the steel beam and 25mm below the bottom of the steel beam.

For the continuous beam type specimen, the strain reached the yield strain at R=0.01rad rotation angle. It rose thereafter. Parts for which the strain rose were only those just above and below the I-section beam. The strain at the edge remained a small value. This tendency is the same as the range of minus rotation angle. The column flanges of the continuous beam type specimen might be affected by the local deformation from the steel beam under bending induced beam tension. However, such effects were not observed in practice until late in the test after extensive beam plastic action had occurred. Local deformation of the column flange above or below the I-section beam becomes large in a tensile region but remains a small value in a compression region, which indicates that the filled concrete contributes greatly to the transmission of the compressive load at the connection panel.

For the orthogonal direction to continuous beam specimen, the strain rise was also observed above and below the beam. The increase of the strain was larger than that of the continuous beam type specimen after R=0.02rad. However, this is due to the out-of-plane deformation of the column flange caused by tensile force from a beam flange and also the lower lever arm between the column centreline and the end of the orthogonal beam web where it sits inside the continuous beam flange.

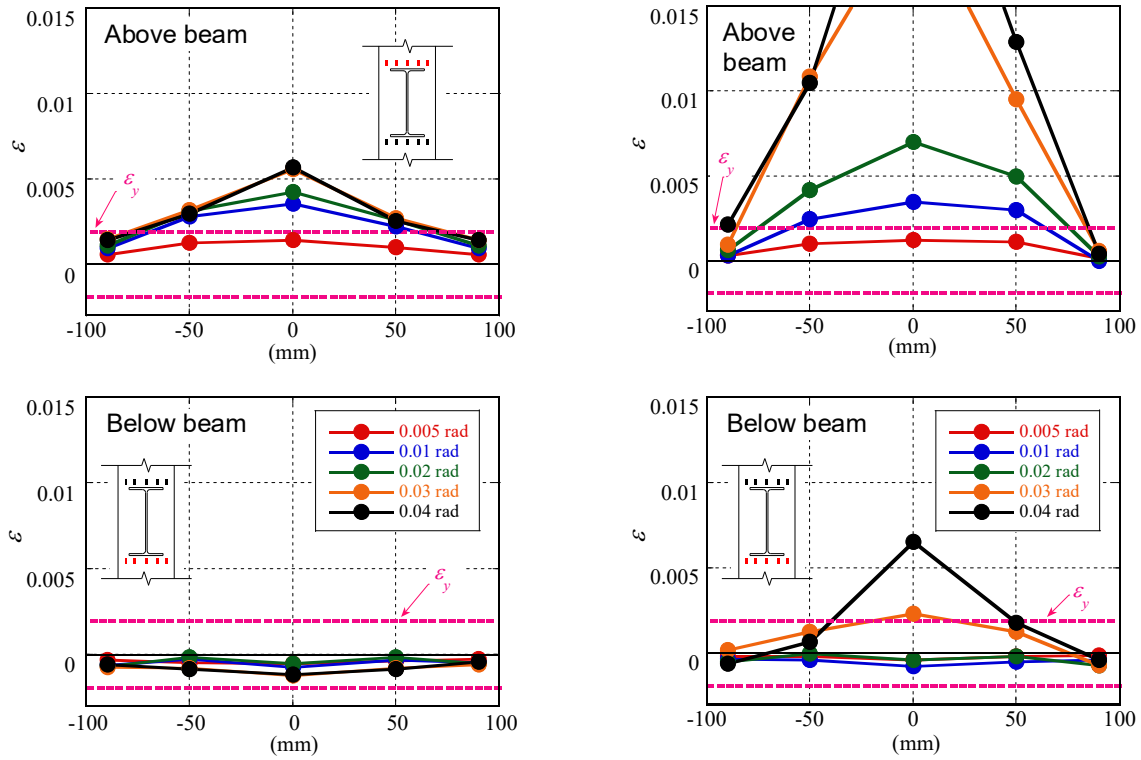

(a) Continuous Beam Type (b) Orthogonal Direction to Continuous Beam

Fig. 8 – Strain Distribution at Steel Tube Flange

4. Concluding remarks

1) A continuous I section beam to CFST column specimen showed good performance with stable behaviour and high energy-absorbing capacity. The maximum experimental strength exceeded the calculated value.

2) For the continuous beam type specimen, the column flange might be affected easily by local deformation from the steel beam under tensile conditions. However, local buckling of the steel column flange was not observed until the end of loading. Filled concrete contributes to transmission of the compressive load at the connection panel.

3) For the orthogonal direction to the continuous beam detail proposed herein, the connection exhibited slightly pinched hysteresis during a small rotation angle, but exhibited stable hysteretic behaviour thereafter, with an increased strength under high rotation. The increase of strength is very likely caused by the inserted beam web contacting the continuous beam flange, enabling greater lever action to develop bending moment. Reducing the clearance between the orthogonal beam shear tab and the inside of the continuous beam flanges will reduce the pinching effect at lower rotations.

5. Acknowledgements

This work was supported by JSPS Grant No. R2904 in the Program for Fostering Globally Talented Researchers. The authors would like to thank Ms. Mizuho Murata for the help with experiments.

6. References

[1] Architectural Institute of Japan (2008): *Recommendations for Design and Construction of Concrete Filled Steel Tubular Structures*, 2nd edition.

[2] Azizinamini A, Prakash BA (1993): Tentative Design Guideline for a New Steel Beam Connection Detail to Composite Tube Columns, *Engineering Journal*, AISC, **30**, 108-115.

[3] Azizinamini A, Schneider SP (2004): Moment Connections to Circular Concrete-Filled Steel Tube Columns, *Journal of Structural Engineering*, **130** (2), 213-222.

[4] Schneider SP, Alostaz YM (1998): Experimental Behavior of Connections to Concrete-Filled Steel Tubes, *Journal of Construction Steel Research*, **45** (3), 321-352.

[5] Fujinaga T, Clifton CG (2019): Experimental Study on Continuous Beam Type Square CFST Beam-to-Column Connection, *Interdependence between Structural Engineering and Construction Management*, *10th International Structural Engineering and Construction Conference*, Chicago, USA.

